Progressive Motor Deficit is Mediated by the Denervation of Neuromuscular Junctions and Axonal Degeneration in Transgenic Mice Expressing Mutant (P301S) Tau Protein

Yin, Zhuoran; Valkenburg, Femke; Hornix, Betty E; Mantingh-Otter, Ietje; Zhou, Xingdong; Mari, Muriel; Reggiori, Fulvio; Van Dam, Debby; Eggen, Bart J L; De Deyn, Peter P

Published in:
Journal of Alzheimer's Disease

DOI:
10.3233/JAD-161206

Journal of Alzheimer's Disease 60 (2017) S41–S57
DOI 10.3233/JAD-161206
IOS Press

Progressive Motor Deficit is Mediated by the Denervation of Neuromuscular Junctions and Axonal Degeneration in Transgenic Mice Expressing Mutant (P301S) Tau Protein

Zhuoran Yin[a,b,1], Femke Valkenburg[c,1], Betty E. Hornix[d], Ietje Mantingh-Otter[a], Xingdong Zhou[e,f], Muriel Mari[e], Fulvio Reggiori[e], Debby Van Dam[c,g], Bart J.L. Eggen[a], Peter P. De Deyn[c,g,h] and Erik Boddeke[a,*]

[a]*Department of Neuroscience, Section Medical Physiology, University Medical Center Groningen, University of Groningen, Groningen, The Netherlands*
[b]*Department of Medical Ultrasound, Tongji Hospital, Tongji Medical College, Huazhong University of Science and Technology, Wuhan, China*
[c]*Laboratory of Neurochemistry and Behavior, Institute Born-Bunge, University of Antwerp, Antwerp, Belgium*
[d]*Department of Neurobiology, Groningen Institute for Evolutionary Life Science, University of Groningen, Groningen, The Netherlands*
[e]*Department of Cell Biology, University Medical Center Groningen, University of Groningen, Groningen, The Netherlands*
[f]*Department of Preventive Veterinary Medicine, College of Veterinary Medicine, Northeast Agricultural University, Harbin, China*
[g]*Department of Neurology and Alzheimer Research Center, University Medical Center Groningen, University of Groningen, Groningen, The Netherlands*
[h]*Biobank, Institute Born-Bunge, Antwerp, Belgium*

Accepted 23 January 2017

Abstract. Tauopathies include a variety of neurodegenerative diseases associated with the pathological aggregation of hyperphosphorylated tau, resulting in progressive cognitive decline and motor impairment. The underlying mechanism for motor deficits related to tauopathy is not yet fully understood. Here, we use a novel transgenic tau mouse line, Tau 58/4, with enhanced neuron-specific expression of P301S mutant tau to investigate the motor abnormalities in association with the peripheral nervous system. Using stationary beam, gait, and rotarod tests, motor deficits were found in Tau 58/4 mice already 3 months after birth, which deteriorated during aging. Hyperphosphorylated tau was detected in the cell bodies and axons of motor neurons. At the age of 9 and 12 months, significant denervation of the neuromuscular junction in the extensor digitorum longus muscle was observed in Tau 58/4 mice, compared to wild-type mice. Muscle hypotrophy was observed in Tau 58/4 mice at 9 and 12 months. Using electron microscopy, we observed ultrastructural changes in the sciatic nerve of 12-month-old Tau 58/4 mice indicative of the loss of large axonal fibers and hypomyelination (assessed by g-ratio). We conclude that the accumulated hyperphosphorylated tau in the axon terminals may induce dying-back axonal degeneration,

[1]These authors contributed equally to this work.

*Correspondence to: Erik Boddeke, Department of Neuroscience, Section Medical Physiology, University Medical Center Groningen, Antonius Deusinglaan 1, Groningen, 9713 AV, The Netherlands. Tel.: +31 503616443; Fax: +31 503632751; E-mail: h.w.g.m.boddeke@umcg.nl.

myelin abnormalities, neuromuscular junction denervation, and muscular atrophy, which may be the mechanisms responsible for the deterioration of the motor function in Tau 58/4 mice. Tau 58/4 mice represent an interesting neuromuscular degeneration model, and the pathological mechanisms might be responsible for motor signs observed in some human tauopathies.

Keywords: Alzheimer's disease, axonal degeneration, motor dysfunction, neuromuscular junction denervation, tauopathy

INTRODUCTION

Tauopathies comprise various neurodegenerative diseases characterized by the pathological accumulation of hyperphosphorylated microtubule-associated protein tau (MAPT) in the nervous system. Most tauopathies, including Alzheimer's disease (AD), frontotemporal dementia with parkinsonism linked to chromosome 17 (FTDP-17), progressive supranuclear palsy (PSP), and corticobasal degeneration (CBD) cause dementia or degeneration of the motor system [1]. In AD, motor signs have been described in long term follow-up of large AD cohorts. Some of the motor signs are due to mixed pathologies and/or the involvement of neuropathological lesions in substantia nigra, striatum, and mesocortical pathways, etc. [2, 3]. FTDP-17, PSP, and CBD share some motor deficits with Parkinson's disease including bradykinesia, tremors, and rigidity, which occur at an early stage of the disease [4]. Until now, no symptomatic treatment for FTDP-17, CBD, or PSP has been approved by the US Food and Drug Administration. Off-label use of symptomatic medication for motor symptoms such as levodopa is based on clinical experience [5], but the percentage of levodopa resistance in tauopathies remains high [5, 6]. Loss of dopaminoreceptive neurons in substantia nigra may be one of the reasons for the levodopa-resistant motor dysfunction in tauopathy [7]. Disturbance of axonal transport has also been indicated as a possible mechanism for motor deficits in transgenic tauopathy mouse models [8]. Clearly, further research on peripheral nerve pathology and motor function in tauopathies is required to better understand the underlying mechanisms and to provide new therapeutic possibilities for motor impairment in tauopathy.

Tau, as one of the major microtubule-associated proteins, is important for stabilization of microtubules and maintenance of axoplasmic flow [9]. Several mutations in the tau gene have been identified in FTDP-17 families, e.g., exon 10 (P301L, P301S, N279K), exon 9 (G257T, G272V), exon 12 (V337M), or exon 13 (R406W) [10], which all appear to alter the conformation of the protein. Consequently, mutant tau has a higher affinity for brain protein kinases, phosphorylates at a faster rate, self-aggregates more easily into paired helical filaments and, subsequently, into neurofibrillary tangles [9]. Abnormal accumulation of hyperphosphorylated tau leads to pathological alterations in neuronal structures including dystrophic neurites observed in AD, which is characterized by the disorganization of the microtubule- and neurofilament network [11]. Hyperphosphorylated tau can disassemble microtubules, which may block axoplasmic flow and induce retrograde neuronal degeneration [9]. Restoration of microtubule stabilization has been demonstrated to improve axonal transport and motor symptoms in transgenic tau mice [12]. Axonal transport could, therefore, be a future therapeutic target for tauopathy [13].

Various transgenic mouse models for tau pathology have been generated [14], which show many features of human tauopathy. Expression of FTDP-17-related (e.g., P301L/S, V337M, and R406W) mutant tau proteins in transgenic mice, induces symptoms of human tauopathy, such as motor disturbances and memory loss [14–16]. Loss of functional synapses and axon degeneration were also observed in transgenic tau mouse models [8, 17, 18]. The phenotype of tau mouse models depends on the tau mutation, promoters, and tau isoform composition [15, 17, 19]. Understanding pathological alterations and phenotypic changes in tau transgenic mouse models may provide new insight into the onset and development of human tauopathy [17].

The current study focuses on a novel mouse model Tau 58/4, which contains the point mutation P301S in exon 10 of the human MAPT gene under regulation by the neuron-specific Thy-1.2 promoter. As a consequence, mutant tau proteins distribute both in neuronal somata and axonal compartments. A battery of motor tests, including gait analysis, the stationary beam test, the hindlimb clasping test, and rotarod performance were applied to evaluate the motor function of Tau 58/4 mice. By immunofluorescence staining, the percentage of partially innervated and denervated neuromuscular junctions was quantified in the extensor digitorum longus (EDL) muscle. Using electron microscopy, ultrastructural alterations of axons were observed in the sciatic nerve of 12-month-old Tau 58/4 mice. Our data suggest that the expression of human transgenic tau in the motor

neurons impairs axonal function and the maintenance of neuromuscular junctions. Subsequently, it leads to muscle denervation, which could be one of the underlying mechanisms of the deteriorating motor function observed during aging in Tau 58/4 mice.

MATERIALS AND METHODS

Tau 58/4 transgenic mice

Generation of transgenic mice was performed as described preciously [20]. Briefly, to create the Tau58/4 construct, a F115 TAU cDNA encoding the human tau isoform (0N4R) containing the P301S mutation was cloned into the pTSC21K bacterial expression vector including the murine Thy1.2 gene [21] using the XhoI restriction site. Vector sequences were removed by NotI PvuI digestion. Injection and manipulation of mice was identical to described procedures [20]. Tau 58/4 mice were generated in a hybrid C57BL/6 × DBA2 background, and then the mice were backcrossed to C57BL/6J to create an isogenic line. The 58/4 transgenic line is fertile and produces normal sized litters. Only heterozygous, male mice were used for experiments.

Mice were weaned 4 weeks after birth and group housed with littermates of the same sex. Food and water were supplied *ad libitum*. Custom primers were used for genotyping by PCR analysis with ear punches, collected from mice aged approximately 4 weeks, as source of DNA. Motor tests and surgical procedures were performed during the light phase of the animals, and all mice were acclimatized for at least 1h before conducting the experiments. Experimenters were blinded to the genetic status of the animals. All experiments were carried out in compliance with the European Community Council Directive (2010/63/EU) and were approved by the Animal Ethics Committee of the University of Antwerp (ECD 2013–31).

Behavioral tests

Male heterozygous (HET) mice and wild-type (WT) control littermates aged 3, 6, 9, and 12 months were subjected to a battery of motor function-related behavioral tests. The numbers of used animals are listed in Table 1.

Hindlimb clasping test

Animals were suspended by the tail and kept at a height of 40 cm above the able top for a duration of 30 s, during which the presence of hindlimb clasping behavior was observed.

Gait analysis

Gait characteristics (stride length, toe span, and track width) were analyzed by applying ink to the hind paws of the animals. Mice were then allowed to walk on a strip of paper in a brightly lit walk lane (width: 4.5 cm, length: 40 cm), toward a dark goal box. At least 2 complete gait patterns from each mouse were obtained on which gait characteristics were measured by caliper.

Stationary beam test

The stationary beam test of equilibrium and balance was performed on a wooden beam (diameter: 25 mm, length: 110 cm) covered with a layer of masking tape to provide a firm grip. The beam was divided into 11 segments and placed at a height of 38 cm above a cushioned bench. The ends of the beam

Table 1
Motor function-related parameters obtained with the tests applied to assess the motor function of the Tau 58/4 mice in comparison with age-matched WT littermates

Tau 58/4	Age	3 months		6 months		9 months		12 months	
	Genotype	WT ($n=9$)	HET ($n=10$)	WT ($n=11$)	HET ($n=11$)	WT ($n=11$)	HET ($n=12$)	WT ($n=15$)	HET ($n=16$)
Stationary Beam test									
Number of segments		60 ± 9	20 ± 3**	48 ± 8	14 ± 6**	42 ± 10	10 ± 5*	25 ± 6	6 ± 2*
Number of falls		0.2 ± 0.1	1.5 ± 0.5*	0.5 ± 0.3	0.9 ± 0.3	0	1.8 ± 0.4**	0.5 ± 0.2	2.3 ± 0.3***
Latency to first fall (s)		232 ± 6	211 ± 10	217 ± 14	201 ± 11	233 ± 7	169 ± 19**	222 ± 7	141 ± 15***
Gait Analysis									
Stride length left (mm)		63 ± 3	62 ± 2	62 ± 2	49 ± 2***	69 ± 2	50 ± 2***	72 ± 2	47 ± 1***
Stride length right (mm)		65 ± 3	60 ± 2	62 ± 2	50 ± 2***	69 ± 2	49 ± 1***	74 ± 1	46 ± 1***
Toespan left (mm)		8.51 ± 0.18	8.44 ± 0.19	8.48 ± 0.24	8.26 ± 0.17	7.64 ± 0.2	7.91 ± 0.16	8.13 ± 0.12	8.26 ± 0.14
Toespan right (mm)		8.2 ± 0.22	8.14 ± 0.25	8.77 ± 0.15	7.9 ± 0.17**	7.89 ± 0.11	7.73 ± 0.19	7.3 ± 0.25	7.9 ± 0.17
Width (mm)		26 ± 1	26 ± 0.4	29 ± 1	28 ± 0.4	29 ± 0.5	28 ± 1	29 ± 0.4	27 ± 1*

Data are presented as mean ± S.E.M. Statistical significance was determined with the two-tailed Student's *t*-test. *$p<0.05$, **$p<0.01$, ***$p<0.001$. WT, wild type; HET, heterozygous.

were shielded with cardboard to prevent the mice from escaping. Testing commenced by placing an animal in the middle of the beam. The number of segments crossed (four-paw criterion), the latencies before falling, and the number of falls were measured for four trials with a cut-off period of 1 min per trial and an intertrial interval of 10 min.

Accelerating rotarod

Equilibrium, balance, and motor coordination were tested on an accelerating rotarod apparatus (Panlab, Barcelona, Spain). After two acclimatization trials with a maximum duration of 2 min each at a constant speed (4 rpm), each mouse was placed on the rotating rod for four test trials, during which the rotation speed gradually increased from 4 to 40 rpm (intertrial interval: 1 min). The time an animal remained on the rotating rod was measured during the test trials with a cut-off period of 5 min per trial.

Tissue sampling and embedding

Tau 58/4 and WT mice were anesthetized and transcardially perfused with saline. Spinal cord tissue was removed and cut into cervical, thoracic, lumbar, and sacral segments. Sciatic nerves and EDL muscles were also collected. For immunohistochemistry, spinal cord tissue ($n = 8$) was formalin fixed and embedded in paraffin. Spinal cord tissue ($n = 3$), left sciatic nerve ($n = 5$), and left EDL muscle ($n = 3$–5) were put in 4% PFA in PBS for 1 day, dehydrated with 25% sucrose in PBS overnight at 4°C and then frozen at –50°C. For neuromuscular junction innervation analysis, right EDL muscle ($n = 3$–4) was snap frozen in 2-methylbutane, which was kept on dry ice (–40°C) and then stored at –80°C.

For electron microscopy, the right sciatic nerve ($n = 5$) was cut into 2 mm-long pieces, and fixed with 2% PFA and 2.5% glutaraldehyde in 0.1 M PHEM buffer (20 mM PIPES, 50 mM HEPES, pH 6.9, 20 mM EGTA, 4 mM $MgCl_2$) at room temperature [22] for 3 h. Samples were washes 3 times with 0.1 M PHEM buffer before being post-fixed in 1% osmium tetroxide and 1% potassium ferricyanide in 0.1 M PHEM buffer at 4°C for 90 min. Samples were then embedded in Epon resin as previously described [23].

Immunohistochemistry

Coronal sections of thoracic spinal cord and sagittal sections of sacral spinal cord (5 μm, paraffin-embedded) of Tau 58/4 mice at the age of 6 and 12 months were cut for immunohistochemical staining. The sections were firstly deparaffinized in xylene and ethanol. The sections were subsequently pre-incubated in 1% H_2O_2 for 30 min. After washing in TBS, the sections were blocked for 30 min with 4% normal swine serum in TBS + 1% bovine serum albumin (BSA). Sections were then incubated at 4°C overnight with primary antibody (AT8, 1:10000, produced by Institute Born-Bunge, University of Antwerp) in TBS + 1% BSA. After TBS washing, the sections were incubated with biotinylated anti-mouse IgG (1:200, Amersham, RPN1001) in TBS + 1% BSA at room temperature for 30 min. Next, all the sections were washed with TBS and incubated in avidin-biotin-peroxidase complex (Vectastain ABC kit, Vector Laboratories, PK-6100) for 30 min and visualized with 3, 3′-diaminobenzidine (DAB, Sigma, D-5637).

Coronal sections of the lumbar spinal cord (14 μm for sections on glass slides, 40 μm for free floating tissue) of Tau 58/4 and WT mice at the age of 3, 9, and 12 months were pre-incubated in 0.3 % H_2O_2 in PBS for 30 min (only for light microscopy). Then the sections were blocked with 10 % normal serum. Sections were incubated overnight at room temperature with the primary antibodies: NeuN (1:500, Abcam, EPR12763), AT8 (1:10000, Antwerp), Mac-2 (1:1000, Cedarlane, CL8942AP), GFAP (1:1000, DAKO, Z0334). After PBS washing, for light microscopy, sections were incubated with biotinylated secondary antibodies for 1 h (goat anti-rabbit IgG, 1:400, Vector Laboratories, BA-1000; rabbit anti-rat IgG, 1:400, Vector Laboratories, BA-4001; horse anti mouse IgG, 1:400, Vector Laboratories, BA-2000) followed by addition of the avidin-biotin-peroxidase complex (Vector Laboratories, PK-6100) for 30 min and visualized with DAB. The sections were mounted with Depex (Sigma, 06522). For fluorescence microscopy, sections were incubated in donkey anti-rabbit Alexa 488 (1:400, ThermoFisher, A-21206) and donkey anti-rat Cy3 (1:400, JIR, 712–165–150). The sections were mounted with Mowiol (Calbiochem, 475904).

Immunofluorescence labeling of neuromuscular junctions

Snap frozen EDL muscle samples (100 μm for free floating tissue) of Tau 58/4 and WT mice at the age of 3, 9, and 12 months were cut using a cryostat. Muscle sections were incubated in α-bungarotoxin Alexa 594 (1:200, Molecular Probes, B13423) in PBS for 30 min, followed by 4% PFA in PBS for

10 min. The sections were then blocked with 4 % BSA in PBS for 1 h. Sections were incubated in primary antibody neurofilament-M (165 kDa) (1:300, DSHB, 2H3) with 1% BSA in PBS + 0.3 % Triton X-100 for 2 h. After washing in PBS, sections were incubated in donkey anti-mouse AF488 (1:400, Molecular Probes, A21202) with 1% BSA in PBS + 0.3% Triton X-100 for 1 h. After another washing step in PBS, sections were incubated in Hoechst for 3 min and mounted on slides using Mowiol (Calbiochem, 475904).

Imaging techniques

Histochemically stained sections were imaged using a Hamamatsu Nanozoomer (Hamamatsu Photonics). Immunofluorescent stained sections were imaged using a Leica SP8 confocal (Leica Microsystems) using LASAF software. The z-maximum-intensity projection function was used to image the complete neuromuscular junctions in the muscle.

Motor neuron counting

The number of motor neurons in the lumbar spinal cord sections of 3-, 9-, and 12-month-old WT and Tau 58/4 mice were counted after the immunostaining of NeuN ($n = 3$). On both sides of the anterior ventral horn of the spinal cord, motor neurons, identified on the basis of the location and the large size of the cell body, were counted.

Transverse area of muscle fiber measurement

Paraffin-embedded EDL muscles of 3-, 9-, and 12-month-old WT and Tau 58/4 mice were cut (5 μm) and stained with Hematoxylin. The sections were scanned with a Hamamatsu Nanozoomer (Hamamatsu Photonics) and the transverse area of EDL muscles was measured by ImageJ software (100–150 fibers / sample, $n = 3$–5).

Analysis of the innervation of motor endplates

After the immunofluorescence labeling of neuromuscular junctions with neurofilament and α-bungarotoxin, at least 90 neuromuscular junctions per animal ($n = 3$–4) were imaged and quantified. The innervation status of the neuromuscular junction was evaluated by categorizing them as fully innervated when there was complete overlap between the two labels, partially innervated when neurofilament was partially absent at the synaptic junction or denervated in case neurofilament was completely absent at the synaptic junction.

Analysis of axon and myelin structure

Epon-resin-embedded samples were cut into semithin (100 nm) and ultrathin sections (70 nm) using a LEICA ultramicrotome UC7. Semithin sections were colored with toluidine blue and imaged using light microscopy before measuring the diameters of axons. The inner area of axons was measured in Image J, then the diameter was calculated and then the average diameters was extrapolated. Approximately 650–1100 axons were quantified for each sample ($n = 3$).

For electron microscopy, ultrathin sections were stained as previously described [23] and examined in an 80-kV transmission electron microscope (TEM, CM100; FEI). Three independent grids (100 axons/grids) were used to assess the number of degeneration axons in each individual mouse. The g-ratio of axons with intact myelin were assessed. The g-ratio [diameter (axon) / diameter (axon + surrounding myelin)] were also calculated using Image J. Approximately 60–150 fibers was measured per animal ($n = 4$).

Statistical analysis

For the statistical analysis, SPSS version 20.0 and GraphPad Prism 5.0 software were used with the probability level set at 95 %. For comparison between two groups, Student's *t*-test, and non-parametric Mann-Whitney test were used. For comparison of multiple groups, Two-way RM-ANOVA test was performed with a Bonferroni *post hoc* test. The data was considered statistical significant as $*p < 0.05$, $**p < 0.01$, and $***p < 0.001$. In the figures, the *p*-value of the analysis is shown.

RESULTS

Tau 58/4 mice show deteriorating motor dysfunction during aging

To evaluate the coordination of motor function, we examined Tau 58/4 and WT mice in the hindlimb clasping test, gait analysis, stationary beam test, and rotarod test at the age of 3-, 6-, 9-, and 12 months (data listed in Table 1). The degree of hindlimb clasping in mice, when suspended by the tail, is used as an

indicator of the severity of motor dysfunction [24, 25]. WT mice at all indicated ages and Tau 58/4 mice at young ages (i.e., 3 and 6 months) showed a normal extension reflex of the hindlimbs. Tau 58/4 mice of 9 and 12 months old showed typical hindlimb clasping behavior (Fig. 1A). Gait is a general indicator of coordination and muscle function [26]. Gait analysis indicated that the stride length in Tau 58/4 animals is shorter than that in WT control animals. A decrease in the stride length was observed bilaterally, with a significant shorter length visible from 6 months on in the Tau 58/4 strain (Fig. 1B). The stationary beam test was used to detect balance and coordination abnormalities. Tau 58/4 mice of 9 and 12 months old remained significantly shorter on the beam. Tau 58/4 mice of all ages covered a significantly lower number of beam segments, and Tau 58/4 mice of 3, 9, and 12 months old had a significantly higher number of falls, compared to WT animals (Fig. 1C-E). Motor neuron performance and equilibrium were analyzed using an accelerating rotarod (Fig. 1F). In all age groups, significant differences between Tau 58/4 and WT animals were observed for the fourth trial (T4). From the age of 9 months on, significant differences were found for all trials performed. Also, from the age of 3 months, the learning curves differed significantly between Tau 58/4 and WT animals, with the HET animals exhibiting a much flatter learning curve. However, the results found in the rotarod experiment are possibly confounded by the agitated and stressed behavior observed in the Tau 58/4 animals, which resulted in early termination of a trial due to the jumping of the rotarod. This behavior was only this pronounced in the rotarod experiment and did not result in the early termination of the other motor experiments described above.

Human Tau transgenic protein is expressed in the motor neurons of Tau 58/4 mice

In order to investigate the relationship between motor dysfunction and tauopathy in Tau 58/4 mice, we determined tauopathy in the spinal cord and sciatic nerve of Tau 58/4 mice. AT8 antibody, which is specific for the phospho-tau residues Ser202, and Thr205, was used for immunohistochemical staining. The staining was performed on transverse sections of thoracic spinal cord and sagittal sections of the sacral spinal cord of Tau 58/4 mice at 6 months and 12 months (Fig. 2A). In 6-month-old Tau 58/4 mice, phosphorylated tau has mainly accumulated in the axonal processes. At the age of 12 months, the expression of phosphorylated tau was increased and was also observed in the somatic compartments of motor neurons of the ventral horn (Fig. 2A). To detect the accumulation of tau-induced neuronal loss, the numbers of motor neurons were counted in the lumbar spinal cord of Tau 58/4 and WT mice at the age of 3, 9, and 12 months. No significant differences in motor neuron numbers were observed between Tau 58/4 and WT mice at all ages (Fig. 2B, C). In the sciatic nerve, enhanced expression of AT8 was observed in 9-month-old Tau 58/4 mice but not in WT mice (Fig. 2D).

Tau 58/4 mice show muscle hypotrophy during aging

To investigate the development of muscular atrophy, transverse sections of EDL muscles of WT and Tau 58/4 mice were stained with hematoxylin. Transverse areas were measured and grouped into separate regions according to size (Fig. 3A, B). The percentage of muscle fiber numbers in different regions was compared between WT and Tau 58/4 mice. At the age of 3 months, the distribution of fiber size in WT and Tau 58/4 mice is similar. At the age of 12 months, 94.5 % fibers of Tau 58/4 mice belong to smaller area regions (i.e., fiber area $< 150\ \mu m^2$), compared to WT mice, which indicated hypotrophy of muscle in Tau 58/4 mice (Fig. 3A, B). The average area of muscular fibers was also compared between WT and Tau 58/4 mice at different ages. At the age of 3 and 9 months, no significant differences were observed. During aging, the average transverse area of EDL fibers in 12-month-old Tau 58/4 mice was significantly smaller than that of WT mice (Fig. 3C).

Tau 58/4 mice show progressive neuromuscular junction denervation during aging

In order to investigate whether the axonal terminals at the neuromuscular junction are early targets for lower motor neuron pathology in Tau 58/4 mice, we analyzed the integrity of the neuromuscular junction in EDL muscle from hindlimbs. Based on the innervation of the motor endplate, neuromuscular junctions were grouped into fully innervated, partially innervated, and denervated junctions (Fig. 4A). At 3 months, the innervation of the motor endplate in WT and Tau 58/4 mice was not significantly different. In 12-month-old Tau 58/4 mice, there was widespread endplate denervation. This was evident by degeneration of presynaptic motor nerve terminals that had

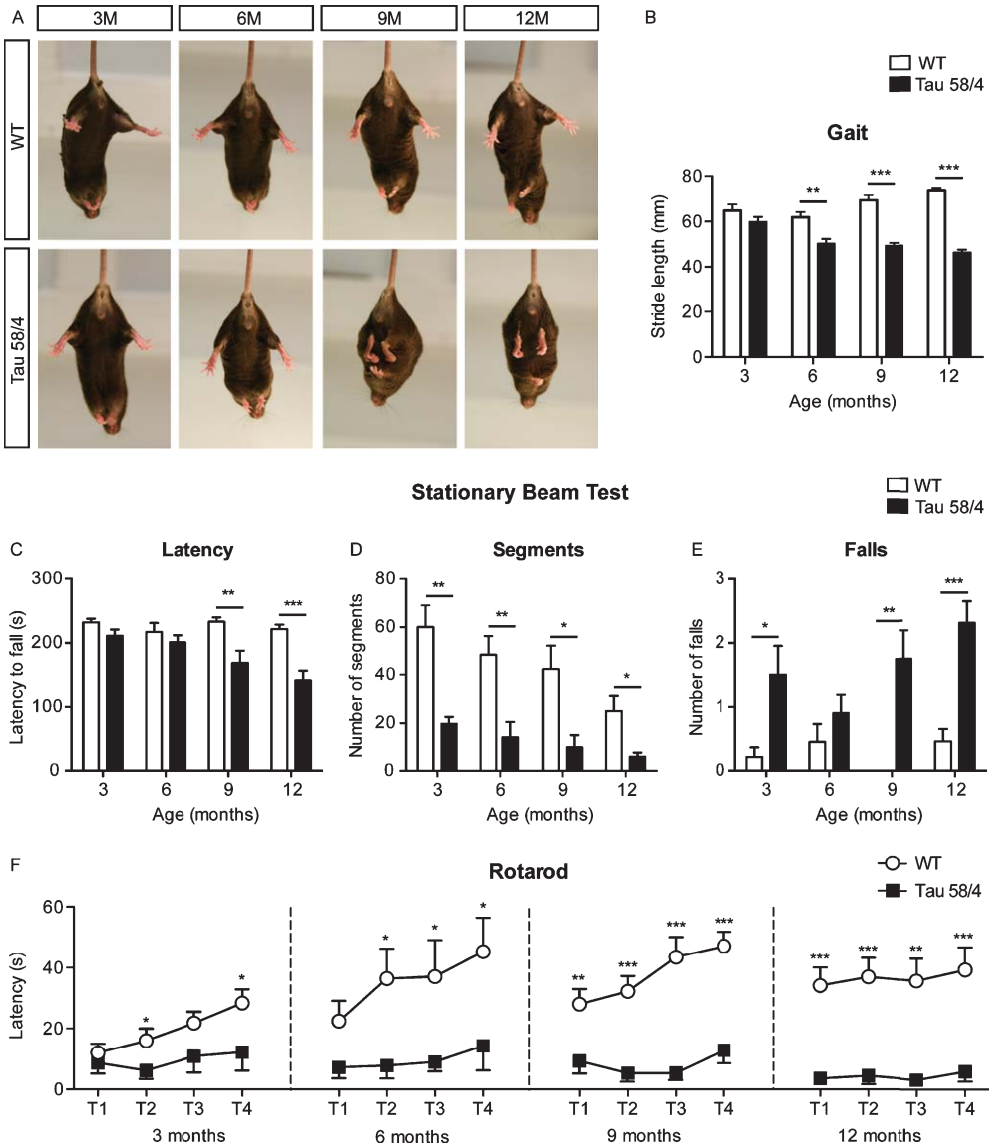

Fig. 1. Motor dysfunction deteriorates in Tau 58/4 mice during aging. A) Representative postures of Tau 58/4 and wild-type (WT) mice in the hindlimb clasping test at the age of 3, 6, 9, and 12 months. WT mice of all ages and Tau 58/4 mice of 3 and 6 months old showed a normal extension reflex in the hindlimbs. However, hindlimb clasping was observed in Tau 58/4 HET animals at the age of 9 and 12 months. B) Gait analysis was performed in Tau 58/4 mice and WT mice at the age of 3, 6, 9, and 12 months. Tau 58/4 mice of 6, 9, and 12 months old showed a shorter stride length compared to WT control mice. Indicated in this figure is the stride length of the right side of the animal and no significant difference was observed between the right and the left stride lengths. Most prominent differences were observed in 12-month-old mice ($p < 0.001$). C-E) Stationary beam testing was performed in Tau 58/4 mice and WT mice at the age of 3, 6, 9, and 12 months. Tau 58/4 mice scored inferior for all measured parameters (the number of covered segments and falls and the duration until the first fall), indicating an impairment in motor function and equilibrium. For Tau 58/4 animals, a significant reduction was observed in the number of covered segments of all age groups [3 months ($p = 0.002$), 6 months ($p = 0.003$), 9 months ($p = 0.010$), and 12 months ($p = 0.010$)]. The number of falls from the beam was increased in Tau 58/4 animals as well [3 months ($p = 0.022$), 9 months ($p = 0.002$), and 12 months ($p < 0.001$)]. The latency to fall was significant shorter in Tau 58/4 animals of 9 months old ($p = 0.007$) and for mice aged 12 months ($p < 0.001$). F) Rotarod results for Tau 58/4 and WT mice at the age of 3, 6, 9, and 12 months. WT animals scored significantly better in the test phase (4 trials, T1, T2, T3, and T4, with a 5-min acceleration to 40 rpm). 3 months: WT $n = 9$, HET $n = 10$; 6 months: WT $n = 11$, HET $n = 11$; 9 months: WT $n = 11$, HET $n = 12$; 12 months: WT $n = 15$, HET $n = 16$; Mean $\pm$ SEM; All age groups: Two-way RM-ANOVA with Bonferroni *post hoc* comparison; Each individual time point: Student's *t*-test, two-tailed, $^{*}p < 0.05$; $^{**}p < 0.01$, and $^{***}p < 0.001$.

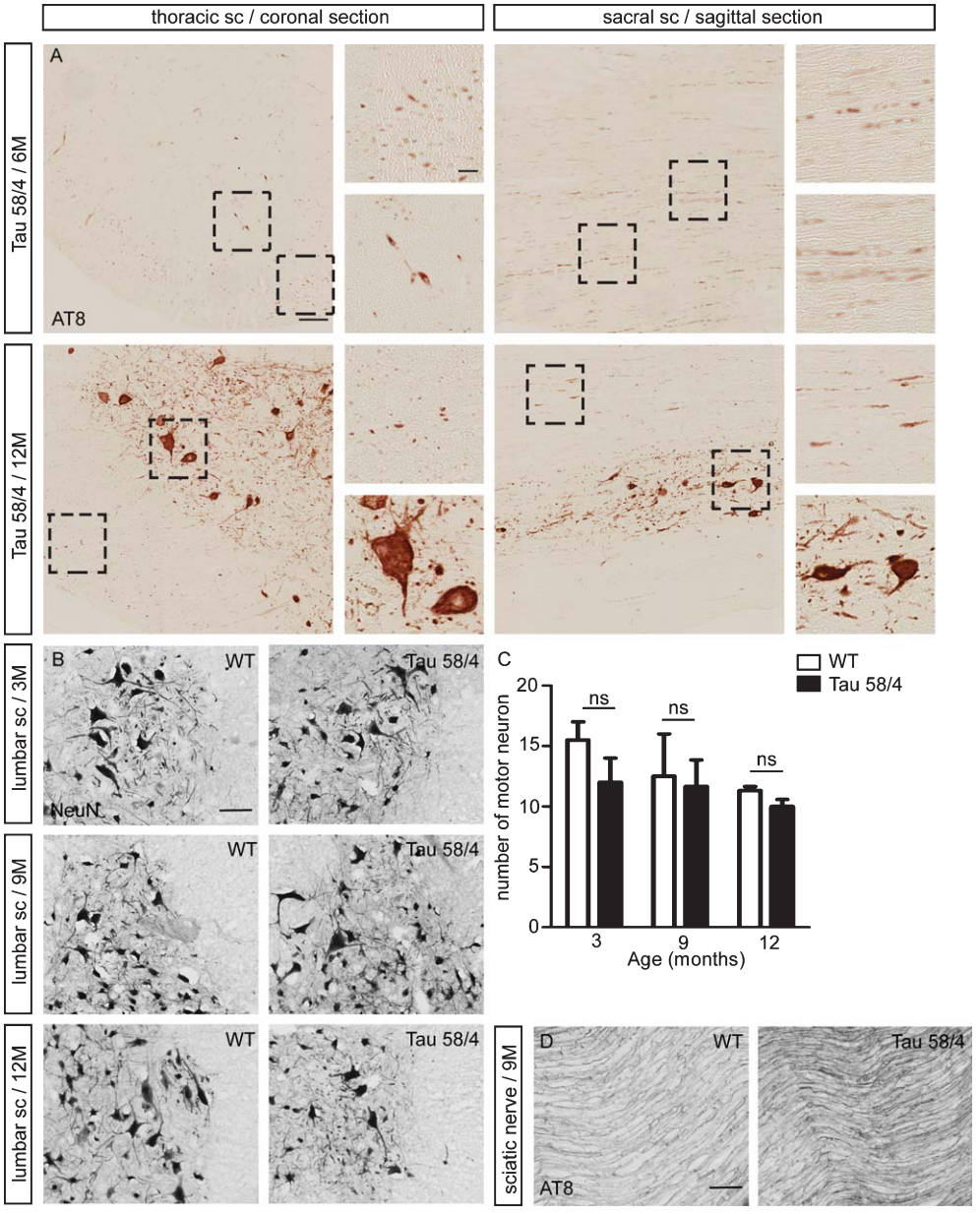

Fig. 2. Tau pathology develops in the spinal cord of Tau 58/4 mice with aging. A) The spinal cord of Tau 58/4 mice at the age of 6 or 12 months was immunostained with AT8 antibody, specific for human mutant tau. The expression of AT8 increased with aging. Magnified pictures show tau pathology in the gray matter and white matter of thoracic spinal cord and sacral spinal cord. B) The spinal cord of WT and Tau 58/4 mice at 3, 9, and 12 months old was immunostained with NeuN. Motor neurons in the anterior horn were clearly identified. C) The number of motor neurons in the lumbar spinal cord of WT (white bar) and Tau (black bar) was quantified at the age of 3, 9, and 12 months. There were no significant differences of motor neuron numbers between WT and Tau 58/4 mice at different ages ($n = 3$, Mean ± SEM, Mann-Whitney test, two-tailed, $^*p < 0.05$). D) The sciatic nerve of 9-month-old WT and Tau 58/4 mice was immunostained with AT8. The expression of phosphorylated tau was higher in Tau 58/4 mice. Scale bars: A = 100 μm, Magnification = 10 μm; B, D = 40 μm.

either entirely or partially disappeared from the post-synaptic motor endplate. Upon aging, there was a decreased percentage of fully innervated endplates and accordingly an increased percentage of partially or completely denervated endplates in Tau 58/4 mice (Fig. 4B). The development of neuromuscular junction denervation during aging was accompanied by deteriorating motor dysfunction, which indicated the distal axonal pathology could be a cause of motor deficit of Tau 58/4 mice.

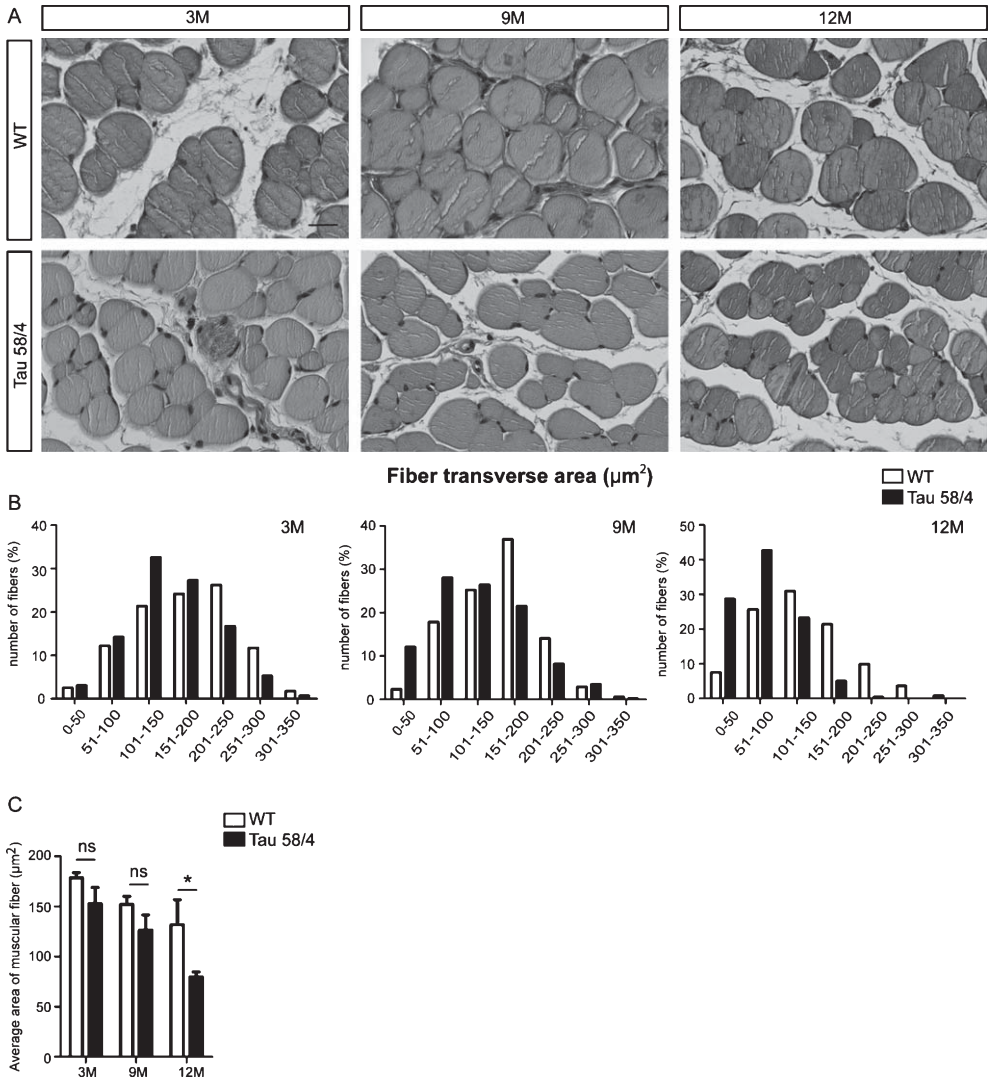

Fig. 3. Muscle hypotrophy in Tau 58/4 mice. A) Hematoxylin staining on transverse sections of extensor digitorum longus (EDL) muscle from 3-, 9-, and 12-month-old WT and Tau 58/4 mice. B) Quantification of transverse area of the muscular fiber of 3-, 9-, and 12-month-old WT (white bar) and Tau 58/4 mice (black bar). At the age of 3 months, the distribution of fiber areas in EDL was similar between WT and Tau 58/4 mice. At the age of 9 months and 12 months, there were significantly reduced proportions of largest muscle fibers in Tau 58/4 mice, compared to WT mice ($n = 3$–5). C) Average area of the transverse section of EDL was compared between WT and Tau 58/4 mice at the age of 3, 9, and 12 months ($n = 3$–5, Mean ± SEM, Mann-Whitney test, two-tailed, $^*p < 0.05$). Scale bar: A = 40 μm.

Ultrastructural analyses reveal axonal degeneration in the sciatic nerve of Tau 58/4 mice

In order to study the structural alterations in myelinated axons of Tau 58/4 mice of 12 months old, we quantified the axon diameter of transverse sections of sciatic nerve stained with toluidine blue (Fig. 5A-D). The average diameter of axons in sciatic nerve was significantly decreased in Tau 58/4 mice (Fig. 5B). The histogram of diameter distribution showed that 89.8% axons of Tau 58/4 mice had a small size (<4 μm), whereas in WT mice the percentage was 75.0% (Fig. 5C). We classified the axons larger than the average diameter of WT mice as "large axons", and those smaller than the average diameter as "small axons". Tau 58/4 mice had a significantly higher percentage of small axons and a significantly lower percentage of large axons, compared to WT mice (Fig. 5D). To evaluate the axonal degeneration of Tau 58/4 mice, we examined the sciatic nerve morphology of WT and Tau 58/4 mice at the age of 12 months using electron microscopy (Fig. 5E).

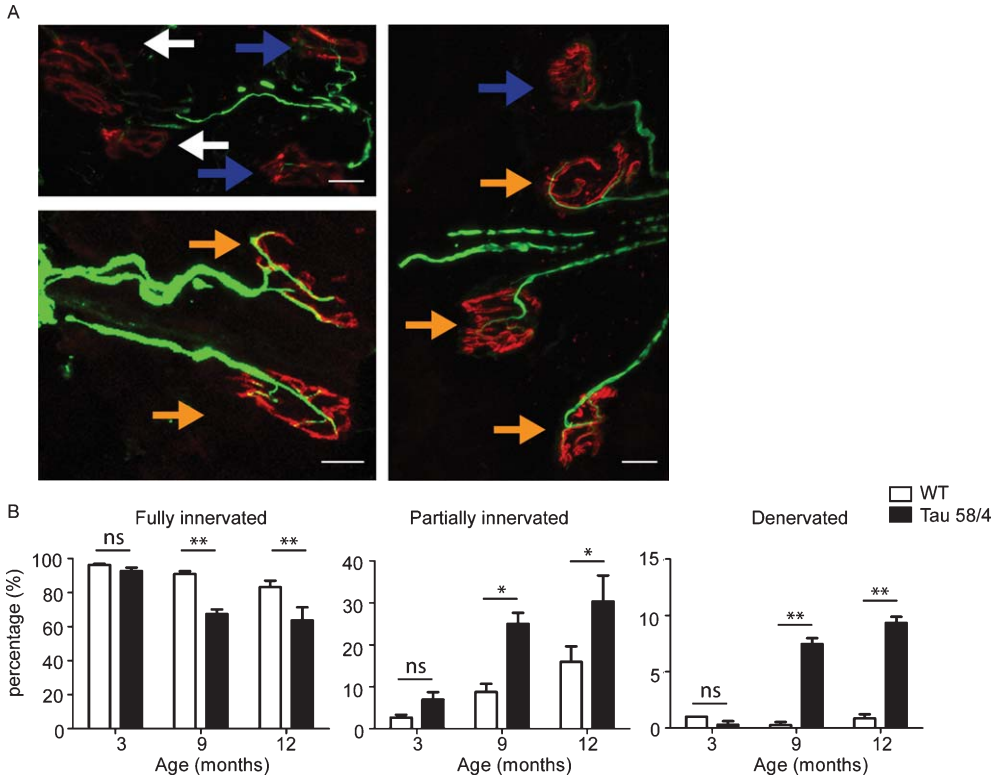

Fig. 4. Expression of human mutant tau protein leads to neuromuscular junction (NMJ) denervation in Tau 58/4 mice. A) The neuromuscular junctions of EDL muscle were immunostained with 165 kDa neurofilament (green) to reveal pre-synaptic axons and motor nerve terminals and labeled with α-bungarotoxin (red) to show post-synaptic motor endplates. Arrows indicate examples of fully innervated (orange arrows), partially innervated (blue arrows), and denervated (white arrows) NMJs. B) Quantification of percentages of fully innervated, partially innervated, and denervated NMJs, comparing 3-, 9-, and 12-month-old WT (white bar) and Tau 58/4 mice (black bar). At the age of 3 months, the percentage of innervated NMJs is similar between WT and Tau 58/4 mice. There is a significantly reduced percentage of fully innervated NMJs and a significantly higher percentage of partially innervated and denervated NMJs in Tau 58/4 mice at the age of 9 and 12 months. (>90 NMJ / animal, $n = 3$–4, Mean ± SEM, Mann-Whitney test, two-tailed, $*p < 0.05$, $**p < 0.01$). Scale bar: A = 20 μm.

We observed proliferation of nonmyelinated axons surrounded by Schwann cells (white arrow) in the sciatic nerve of Tau 58/4 mice. We compared the myelin sheath thickness using the g-ratio, the numerical ratio between the diameter of the axon and the outer diameter of the myelinated fiber. Tau 58/4 mice showed an increasing tendency in g-ratio, which was significantly different in the axons with a diameter of 6–8 μm (Fig. 5F). This observation indicated an hypomyelination of motor-related axons of Tau 58/4 mice [27]. Except the axons with intact myelin sheath (Supplementary Figure 1A), we also observed less electron-dense lines (black arrow) in the myelin sheath of axons (Supplementary Figure 1B) in both WT and Tau 58/4 mice. However, this type of axons was more pronounced in Tau 58/4 animals. Although this was evident, the low frequency of this type of axons did not allow to determine whether this difference was significant (Supplementary Figure 1C). The irregular structures in the myelin sheath might be Schmidt-Lanterman incisura, which is a funnel tube-like cytoplasmic structure that crosses the compact myelin and connects the Schwann cell abaxonal cytoplasm to the adaxonal cytoplasm [28]. However further investigation will be needed to confirm that these structures are Schmidt-Lanterman incisures.

Increased glia activity in the corticospinal tract of spinal cord in Tau 58/4 mice

In order to investigate the involvement of upper motor neurons in the lower motor neuron dysfunction in Tau 58/4 mice, we investigated the glia activity in the corticospinal tract of the spinal cord of Tau 58/4 mice and WT mice. Mac-2, which is a member of the lectin family, has been observed to be upregulated in microglia and astrocytes upon aging and pathological conditions [29]. At the age of 9 and 12 months, we

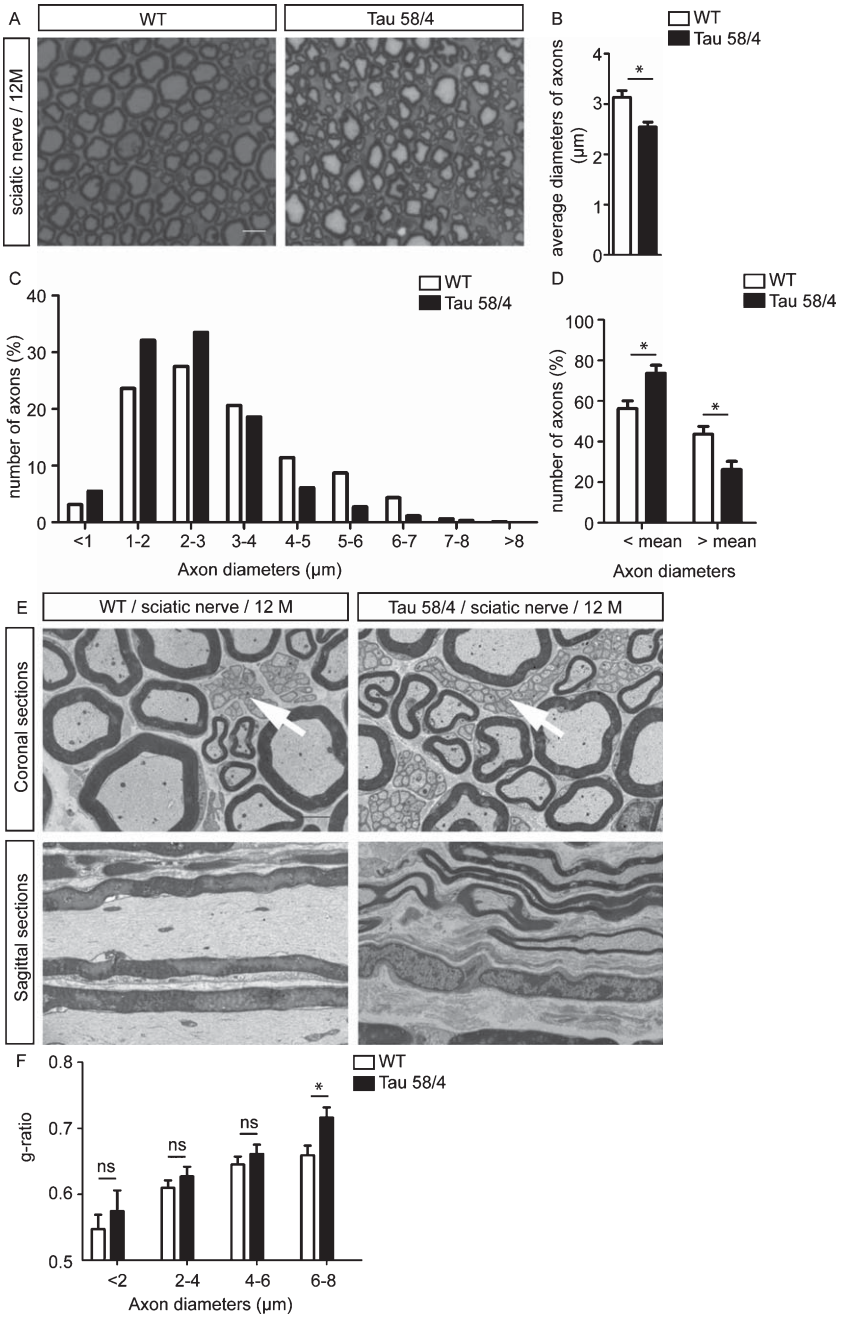

Fig. 5. Ultrastructural features of the sciatic nerve reveal axonal degeneration in Tau 58/4 mice. A) Representative light microscopy photograph of toluidine blue staining of the sciatic nerve of 12-month-old WT and Tau 58/4 mice (650–1100 axons / animal, $n = 3$). B) Quantification of the average transverse diameter of axons in 12-month-old WT (white bar) and Tau 58/4 (black bar). C) The histogram of axon diameters shows more axons of Tau 58/4 mice have a small diameter (<4 µm). D) Compared to the average diameters of WT mice, axons were set as "large axons" and "small axons". Tau 58/4 has a significantly higher percentage of small axons and a lower percentage of large axons. E) Coronal and sagittal ultrathin sections of the sciatic nerve of WT and Tau 58/4 mice at the age of 12 months (white arrows: non-myelinating axons surrounded by Schwann cells). F) Quantification of the g-ratio in the sciatic nerve of 12-month-old WT and Tau 58/4 mice (60–150 axons / animal, $n = 5$, Mean ± SEM, Mann-Whitney test, two-tailed, $^*p < 0.05$). Scale bar: A = 10 µm, E = 2 µm.

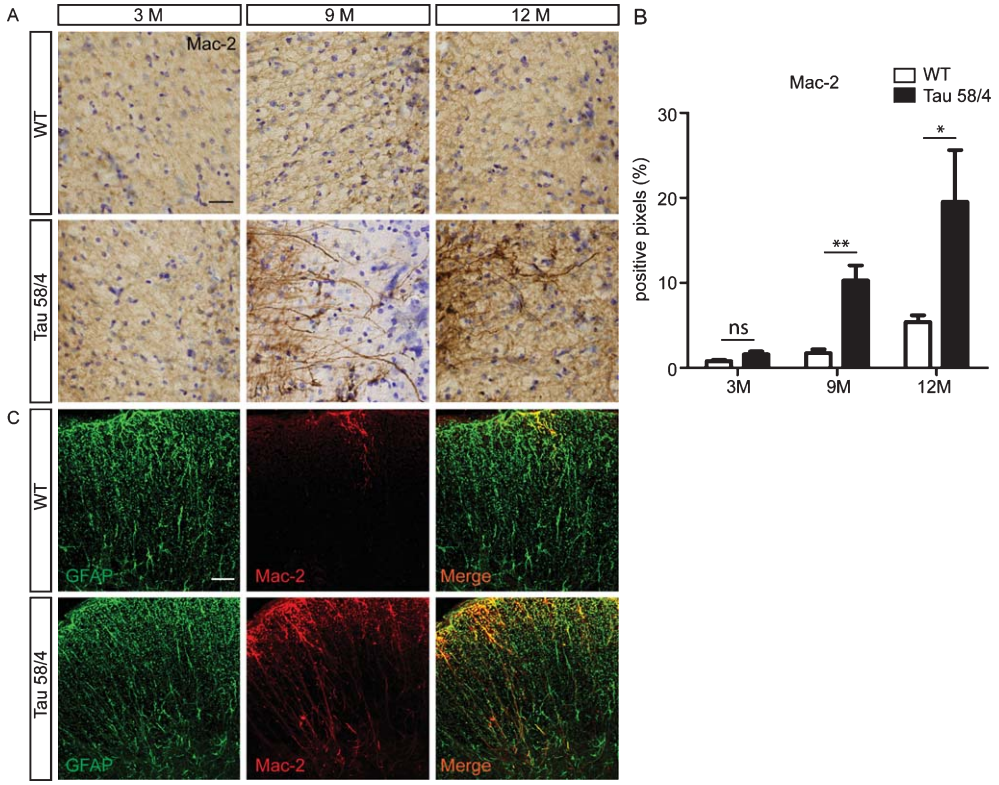

Fig. 6. Astrocyte activation in the lateral corticospinal tract in Tau 58/4 mice. A) Lumbar spinal cord sections of 3-, 9-, and 12-month-old Tau 58/4 and WT mice were immunostained with Mac-2 and counterstained with Cresyl violate. Representative pictures were taken from the region of the lateral corticospinal tract. B) The percentage of positive pixels of Mac-2 in the white matter of lumbar spinal cord, and the expression of Mac-2 was significantly increased in the Tau 58/4 mice of 9- and 12 months old compared to WT ($n = 3$–5, Mean ± SEM, Mann-Whitney test, two-tailed, $^{*}p < 0.05$, $^{**}p < 0.01$). C) Lumbar spinal cord sections of 12-month-old Tau 58/4 and WT mice were immunostained with GFAP and Mac-2. Co-staining were observed between GFAP and Mac-2. Scale bar: A = 25 μm, C = 40 μm.

observed upregulation of Mac-2 in the region of the lateral corticospinal tract of Tau 58/4 mice (Fig. 6A), whereas in 3-month-old mice, this difference was not obvious. The number of Mac-2 positive pixels in Tau 58/4 mice was significantly increased in the white matter regions (Fig. 6B). We also observed co-staining of Mac-2 and GFAP in the region of the lateral corticospinal tract (Fig. 6C), indicative of astrocyte activation in the region of corticospinal tract responding to neuronal changes.

DISCUSSION

In this study, we investigated the motor function and pathological alterations of peripheral nerves in a novel tauopathy mouse model, the Tau 58/4 model. We observed loss of large size peripheral axons, denervation of neuromuscular junctions in 12-month-old Tau 58/4 mice as compared to control littermates. These alterations may lie at the basis of muscle hypotrophy and progressive motor impairment (Fig. 7).

In our study, the stationary beam- and rotarod tests revealed a decline in the motor function already at the age of 3 months. However, rotarod results can be influenced by certain alterations in behavior, such as agitation [30]. Training a highly anxious and agitated animal on the rotarod is much more challenging when compared with calmer animals [31], resulting in an apparently decreased performance of animals that is unrelated to motor function, as described in the PS19 tauopathy mouse model [17]. In previous studies, it was found that rotarod experiments failed to reveal subtle motor alterations, whereas gait analysis and stationary beam tests were more sensitive [32, 33]. Based on the stationary beam tests, the apparent decline in motor functioning in Tau 58/4 mice, starts already at the early age of 3 months. Tau 58/4 mice started to show hindlimb clasping

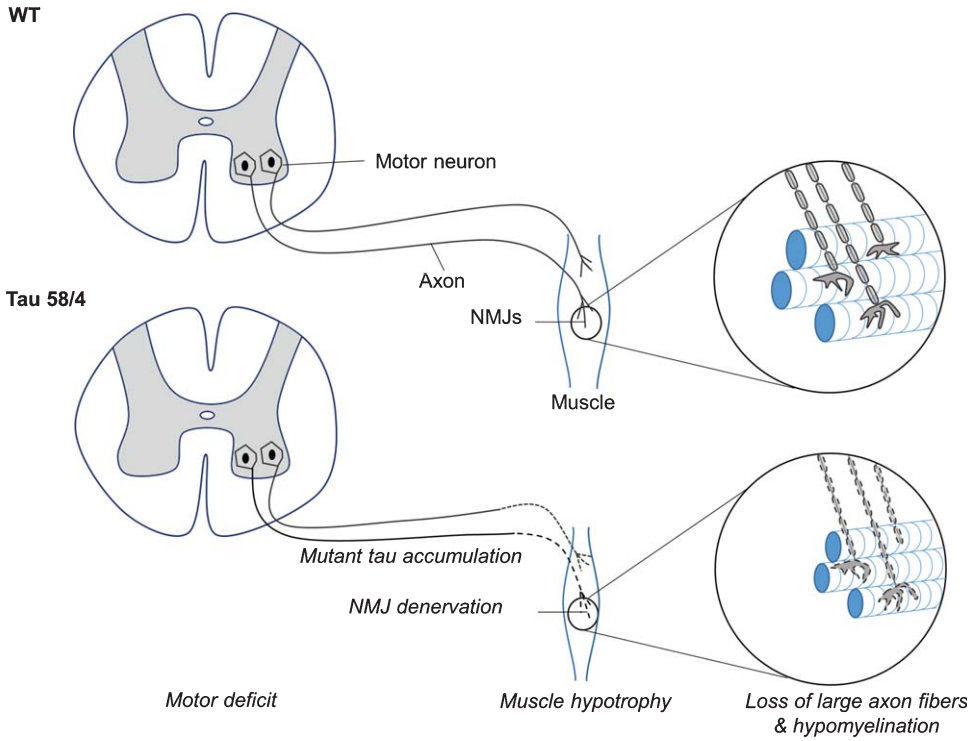

Fig. 7. A schematic representation of hypothetical mechanism for motor deficit in Tau 58/4 mice. In WT mice, motor neurons in the ventral horn of the spinal cord send axons toward the peripheral muscle. Each muscle fiber is innervated by a single motor axon branch. In Tau 58/4 mice, accumulated mutant tau in the axon terminals may induce hypomyelination, loss of large axon fibers, neuromuscular junction denervation, and muscle hypotrophy, which may be the mechanism responsible for motor deficit in Tau 58/4 mice.

behavior at the age of 9 months, which was later than the onset of the motor coordination impairment observed in the rotarod test and stationary beam. We also observed hindlimb muscle hypotrophy at 9 months, which may explain the observed muscle weakness. Previous studies have exposed diverse cognitive and motor phenotypes in various transgenic tauopathy models which may well be due to distinctive pathways of tau molecular pathogenesis and different localization of tau pathology [34]. In PS19 transgenic mice expressing the P301S human T34 tau isoform driven by the mouse prion protein (Prnp) promoter, increased hyperactivity and nociceptive sensitivity, and decreased anxiety-like behavior have been reported [16]. Delayed learning and spatial memory loss have also been found in various transgenic tauopathy mouse models [16, 35, 36]. Motor dysfunction and dystonic posture interference are phenomena observed in transgenic tau mouse models with aggregated mutant tau in axons [8, 34, 37]. However, in the two previously described P301S tauopathy mouse models [17, 38], the motor deficits are so severe that they hinder the age-dependent investigation of specific motor-related functions, as paralysis occurs early in the disease. One exception is the THY-Tau22 model with G272V and P301S mutations, which does not display any motor disturbance [36], although insoluble tau was early (3 months) detected in the axon tracts. In Tau 58/4 mice, mutant tau proteins accumulate both in somata and axonal compartments of motor neurons, and the axonal distribution of mutant tau may be pivotal for the motor impairment. Previous studies in transgenic tau-P301L mouse models indicated that mutant tau mainly aggregated in the soma and dendritic compartments, rather than in axons. Interestingly, no axonal dilations were observed at any age in latter model, and it shows very weak motor symptoms accordingly [39]. In this respect, Tau 58/4 mice represent a straightforward neuromuscular degeneration model.

We observed progressive hypotrophy of muscle fibers and denervation of the neuromuscular junction in aging Tau 58/4 mice. At the age of 9 and 12 months, the muscle hypotrophy accompanied a further decrease in motor dysfunction. This has also been reported in other transgenic tauopathy mouse models

[15, 38]. In Tg30 mice (carrying tau P301S and G272V mutations), two phases of muscular pathology were observed. Initially, muscular hypertrophy was observed at the age of 3 months followed by hypotrophy at the age of 10 months. The muscle hypertrophy at the early age was interpreted as a compensatory mechanism for the degeneration of the nearby muscles and protected the animals from motor dysfunction until 8 months of age [8]. In Tau 58/4 mice muscular hypertrophy was not observed in 3-month-old animals, which may explain the rapid development of motor dysfunction in this model. Neuromuscular junction denervation has been associated with aging [40] and pathological conditions, such as contraction-induced injury [41] and neurodegenerative disorders [42, 43]. In Tau 58/4 mice, the development of neuromuscular junction denervation occurs together with the progression of muscle hypotrophy, which is indicative for denervation-mediated atrophy.

Interestingly, mutant tau also accumulated in the cell body of the motor neurons at the anterior horn of the spinal cord. However, we did not observe a decrease in the number of motor neurons. This suggests that the pathology of the motor neurons follows a distal-to-proximal direction. Axon degeneration in Tau 58/4 mice could be considered to be "dying back degeneration", which has been described previously in chronic neurodegenerative diseases, such as amyotrophic lateral sclerosis [44], spinal muscular atrophy [45], diffuse Lewy body disease [46], and peripheral neuropathy [47]. Generally, this type of chronic axonal degeneration originates from the distal region of the axon and is followed by axon degeneration in a distal-to-proximal direction. The axon subsequently undergoes a progressive fragmentation morphologically resembling Wallerian degeneration [13]. The mechanisms underlying "dying back degeneration" are not fully understood, but mitochondrial dysfunction [48, 49], protein aggregation [49], synaptic pathology [50], disturbance of axonal transport [51, 52], and abnormal activity of autophagy [53] have been previously found to be involved in the process. In Tau 58/4 mice, the neuronal accumulation of mutant tau might be a key player in axonal degeneration. In cultured neurons, aggregated tau inhibits kinesin-dependent transport of organelles, e.g. peroxisomes, mitochondria, and Golgi-derived vesicles into neurites [54]. The inhibition of axonal transport causes oxidative stress, reduces ATP content in synapses and leads to cellular degeneration. Tau could also impair axonal and dendritic ATP transport and thus lead to the accumulation of AβPP in the cell body [54, 55]. The reduction of tau expression does not influence axonal transport under physiological conditions, however, it could prevent Aβ oligomers-impaired axonal motility [56].

In our study, we also observed axonal hypomyelination in the sciatic nerve of 12-month-old Tau 58/4 mice. Axonal demyelination in sciatic nerve has been observed under various pathological conditions including physical injury, chronic inflammatory polyneuropathy, and diabetes [57]. A previous study in myelin-deficient Trembler mice showed a reduction in the rate of slow axonal transport and a slower regeneration rate in demyelinated sciatic nerve [58]. Tau protein plays an important role in the structure and function of myelin. In a recent study, enhanced degenerating, demyelinated fibers and motor impairment in the sciatic nerve of aged Tau -/- mice was observed [27]. Abnormal phosphorylation of tau was associated with both neuronal and axonal loss in animal models of experimental autoimmune encephalomyelitis as well as in human multiple sclerosis [59, 60]. Here, our observations indicate that hyperphosphorylation and accumulation of tau may be associated with axonal degeneration in the peripheral nervous system.

We observed the proliferation of non-myelinating axon surrounded by Schwann cell in the sciatic nerve of 12-month-old Tau 58/4 mice. Schwann cells play an important role in modulation and regenerative support of peripheral axons [58, 61]. Regeneration of non-myelinated axons was also observed after the injury of mammalian peripheral nerve [62]. Previous studies report the non-myelinating Schwann cells distal to nerve injury undergo a large scale change in gene expression, which alters the Schwann cell function from the maintenance of axonal ensheathment to the support of axonal regeneration [63, 64]. Here, the proliferation of non-myelinating Schwann cells may imply an attempt for repair.

Astrocytes play an important role in axon guidance during development and repair [65]. Previous studies have reported progressive astrogliosis and microglia activation in the brain of transgenic Tau mice [17, 66]. Here, we for the first time observed increased Mac-2 expression by astrocytes in the region of the lateral corticospinal tracts in the spinal cord. Mac-2 is a marker associated with the degradation of myelin by microglia, the brain's professional phagocyte, [67] and nonprofessional phagocytes, e.g., astrocyte [68], Schwann cells [69]. The increased number of phagocytic astrocytes might be a response in respect of

clearance of neuronal debris, which may indicate an increased axonal stress from corticospinal tracts or lower motor neurons in Tau 58/4 mice. Future research may aim at the elucidation of the underlying mechanisms.

In this study, we show that accumulation of human tau in axons and cell bodies of motor neurons leads to axonal atrophy and hypomyelination, followed by denervation of neuromuscular junctions and muscular atrophy, leading to impairment of motor functions. The underlying mechanisms of motor deficits in Tau 58/4 mice might be responsible for motor signs observed in some human tauopathies.

ACKNOWLEDGMENTS

We acknowledge Dr. Matthias Staufenbiel for sharing the Tau 58/4 mice line, Prof. Roy Weller, Dr. Wilfred den Dunnen, Dr. Mario Mauthe, Dr. Inge Zijdewind, and Zhuozhao Zhan for useful discussions, and Klaas Sjollema for technical assistance in confocal microscopy. This work was supported by China Scholarship Council (Grant number 201206160050, 2015506610008), Memorable grant from Deltaplan Dementie (Grant number 686180), the Research Foundation-Flanders (FWO), Interuniversity Attraction Poles (IAP) Network P7/16 of the Belgian Federal Science Policy Office, agreement between Institute Born-Bunge and University of Antwerp, the Medical Research Foundation Antwerp, the Thomas Riellaerts research fund, Neurosearch Antwerp, the Belgian Alzheimer Research Foundation (SAO-FRA), and the Alzheimer Research Center of the University Medical Center Groningen (UMCG).

Authors' disclosures available online (http://j-alz.com/manuscript-disclosures/16-1206r1).

SUPPLEMENTARY MATERIAL

The supplementary material is available in the electronic version of this article: http://dx.doi.org/10.3233/JAD-161206.

REFERENCES

[1] Lee VM-Y, Goedert M, Trojanowski JQ (2001) neurodegenerative tauopathies. *Annu Rev Neurosci* **24**, 1121-1159.

[2] Scarmeas N, Hadjigeorgiou GM, Papadimitriou A, Dubois B, Sarazin M, Brandt J, Albert M, Marder K, Bell K, Honig LS, Wegesin D, Stern Y (2004) Motor signs during the course of Alzheimer disease. *Neurology* **63**, 975-982.

[3] Gianutsos JG, Golomb J (1997) Motor/psvchomotor dvsfunction in normal aging, mild cognitive decline, and early Alzheimer's disease: Diagnostic and differential diagnostic features. *Int Psychogeriatrics* **9**, 307-316.

[4] Williams DR (2006) Tauopathies: Classification and clinical update on neurodegenerative diseases associated with microtubule-associated protein tau. *Intern Med J* **36**, 652-660.

[5] Karakaya T, Fußer F, Prvulovic D, Hampel H (2012) Treatment options for tauopathies. *Curr Treat Options Neurol* **14**, 126-136.

[6] Nath U, Ben-Shlomo Y, Thomson RG, Lees AJ, Burn DJ (2003) Clinical features and natural history of progressive supranuclear palsy: A clinical cohort study. *Neurology* **60**, 910-916.

[7] Chiba S, Takada E, Tadokoro M, Taniguchi T, Kadoyama K, Takenokuchi M, Kato S, Suzuki N (2012) Loss of dopaminoreceptive neuron causes L-dopa resistant parkinsonism in tauopathy. *Neurobiol Aging* **33**, 2491-2505.

[8] Audouard E, Van Hees L, Suain V, Yilmaz Z, Poncelet L, Leroy K, Brion JP (2015) Motor deficit in a tauopathy model is induced by disturbances of axonal transport leading to dying-back degeneration and denervation of neuromuscular junctions. *Am J Pathol* **185**, 2685-2697.

[9] Iqbal K, Del C, Alonso A, Chen S, Chohan MO, El-Akkad E, Gong CX, Khatoon S, Li B, Liu F, Rahman A, Tanimukai H, Grundke-Iqbal I (2005) Tau pathology in Alzheimer disease and other tauopathies. *Biochim Biophys Acta* **1739**, 198-210.

[10] Ingram EM, Spillantini MG (2002) Tau gene mutations: Dissecting the pathogenesis of FTDP-17. *Trends Mol Med* **8**, 555-562.

[11] Boutajangout A, Authelet M, Blanchard V, Touchet N, Tremp G, Pradier L, Brion J-P (2004) Characterisation of cytoskeletal abnormalities in mice transgenic for wild-type human tau and familial Alzheimer's disease mutants of APP and presenilin-1. *Neurobiol Dis* **15**, 47-60.

[12] Zhang B, Maiti A, Shively S, Lakhani F, McDonald-Jones G, Bruce J, Lee EB, Xie SX, Joyce S, Li C, Toleikis PM, Lee VM-Y, Trojanowski JQ (2005) Microtubule-binding drugs offset tau sequestration by stabilizing microtubules and reversing fast axonal transport deficits in a tauopathy model. *Proc Natl Acad Sci U S A* **102**, 227-231.

[13] Lingor P, Koch JC, Tönges L, Bähr M (2012) Axonal degeneration as a therapeutic target in the CNS. *Cell Tissue Res* **349**, 289-311.

[14] Lee VM-Y, Kenyon TK, Trojanowski JQ (2005) Transgenic animal models of tauopathies. *Biochim Biophys Acta* **1739**, 251-259.

[15] Lewis J, Mcgowan E, Rockwood J, Melrose H, Nacharaju P, Van M, Gwinn-hardy K, Murphy MP, Baker M, Yu X, Duff K, Hardy J, Corral A, Lin W, Yen S, Dickson DW, Davies P, Hutton M (2000) Neurofibrillary tangles, amyotrophy and progressive motor disturbance in mice expressing mutant (P301L) tau protein. *Nat Genet* **25**, 402-405.

[16] Takeuchi H, Iba M, Inoue H, Higuchi M, Takao (2011) P301S mutant human tau transgenic mice manifest early symptoms of human tauopathies K, Tsukita K, Karatsu Y, Iwamoto Y, Miyakawa T, Suhara T, Trojanowski JQ, Lee VM-Y, Takahashi Rwith dementia and altered sensorimotor gating. *PLoS One* **6**, e21050.

[17] Yoshiyama Y, Higuchi M, Zhang B, Huang SM, Iwata N, Saido T, Maeda J, Suhara T, Trojanowski JQ, Lee VMY (2007) Synapse loss and microglial activation precede tangles in a P301S tauopathy mouse model. *Neuron* **53**, 337-351.

[18] Ishihara T, Hong M, Zhang B, Nakagawa Y, Lee MK, Trojanowski JQ, Lee VM-Y (1999) Age-dependent emergence and progression of a tauopathy in transgenic mice overexpressing the shortest human tau isoform. *Neuron* **24**, 751-762.

[19] Götz J, Chen F, Dorpe J, van, Nitsch RM (2001) Formation of neurofibrillary tangles in P301L tau transgenic mice induced by Aβ42 fibrils. *Science* **293**, 1491-1495.

[20] Andrä K, Abramowski D, Duke M, Probst A, Wiederhold KH, Bürki K, Goedert M, Sommer B, Staufenbiel M (1996) Expression of APP in transgenic mice: A comparison of neuron-specific promoters. *Neurobiol Aging* **17**, 183-190.

[21] Lüthi A, Van der Putten H, Botteri FM, Mansuy IM, Meins M, Frey U, Sansig G, Portet C, Schmutz M, Schröder M, Nitsch C, Laurent JP, Monard D (1997) Endogenous serine protease inhibitor modulates epileptic activity and hippocampal long-term potentiation. *J Neurosci* **17**, 4688-4699.

[22] Schliwa M, Van Blerkom J (1981) Structural interaction of cytoskeletal components. *J Cell Biol* **90**, 222-235.

[23] Verheije MH, Raaben M, Mari M, Te Lintelo EG, Reggiori F, Van Kuppeveld FJM, Rottier PJM, De Haan CAM (2008) Mouse hepatitis coronavirus RNA replication depends on GBF1-mediated ARF1 activation. *PLoS Pathog* **4**, e1000088.

[24] Lei P, Ayton S, Moon S, Zhang Q, Volitakis I, Finkelstein DI, Bush AI (2014) Motor and cognitive deficits in aged tau knockout mice in two background strains. *Mol Neurodegener* **9**, 29.

[25] Zhu J, Li Y, Wang Z, Jia W, Xu R (2016) Toll-like receptor 4 deficiency impairs motor coordination. *Front Neurosci* **10**, 1-10.

[26] Brooks SP, Dunnett SB (2009) Tests to assess motor phenotype in mice: A user's guide. *Nat Rev Neurosci* **10**, 519-529.

[27] Lopes S, Lopes A, Pinto V, Guimaraes MR, Sardinha VM, Duarte-Silva S, Pinheiro S, Pizarro J, Oliveira JF, Sousa N, Leite-Almeida H, Sotiropoulos I (2016) Absence of Tau triggers age-dependent sciatic nerve morphofunctional deficits and motor impairment. *Aging Cell* **15**, 208-216.

[28] Tricaud N, Perrin-Tricaud C, Brusés JL, Rutishauser U (2005) Adherens junctions in myelinating Schwann cells stabilize schmidt-lanterman incisures via recruitment of p120 catenin to E-cadherin. *J Neurosci* **25**, 3259-3269.

[29] Raj DD, Jaarsma D, Holtman IR, Olah M, Ferreira FM, Schaafsma W, Brouwer N, Meijer MM, de Waard MC, van der Pluijm I, Brandt R, Kreft KL, Laman JD, de Haan G, Biber KPH, Hoeijmakers JHJ, Eggen BJL, Boddeke HWGM (2014) Priming of microglia in a DNA-repair deficient model of accelerated aging. *Neurobiol Aging* **35**, 2147-2160.

[30] Spittaels K, Van den Haute C, Van Dorpe J, Bruynseels K, Vandezande K, Laenen I, Geerts H, Mercken M, Sciot R, Van Lommel A, Loos R, Van Leuven F (1999) Prominent axonopathy in the brain and spinal cord of transgenic mice overexpressing four-repeat human tau protein. *Am J Pathol* **155**, 2153-2165.

[31] Balkaya M, Kröber JM, Rex A, Endres M (2012) Assessing post-stroke behavior in mouse models of focal ischemia. *J Cereb Blood Flow Metab* **33**, 330-338.

[32] Stroobants S, Gantois I, Pooters T, D'Hooge R (2013) Increased gait variability in mice with small cerebellar cortex lesions and normal rotarod performance. *Behav Brain Res* **241**, 32-37.

[33] Roth L, Van Dam D, Van der Donckt C, Schrijvers DM, Lemmens K, Van Brussel I, De Deyn PP, Martinet W, De Meyer GRY (2015) Impaired gait pattern as a sensitive tool to assess hypoxic brain damage in a novel mouse model of atherosclerotic plaque rupture. *Physiol Behav* **139**, 397-402.

[34] Melis V, Zabke C, Stamer K, Magbagbeolu M, Schwab K, Marschall P, Veh RW, Bachmann S, Deiana S, Moreau PH, Davidson K, Harrington KA, Rickard JE, Horsley D, Garman R, Mazurkiewicz M, Niewiadomska G, Wischik CM, Harrington CR, Riedel G, Theuring F (2014) Different pathways of molecular pathophysiology underlie cognitive and motor tauopathy phenotypes in transgenic models for Alzheimer's disease and frontotemporal lobar degeneration. *Cell Mol Life Sci* **72**, 2199-2222.

[35] Ramsden M, Kotilinek L, Forster C, Paulson J, McGowan E, SantaCruz K, Guimaraes A, Yue M, Lewis J, Carlson G, Hutton M, Ashe KH (2005) Age-dependent neurofibrillary tangle formation, neuron loss, and memory impairment in a mouse model of human tauopathy (P301L). *J Neurosci* **25**, 10637-10647.

[36] Schindowski K, Bretteville A, Leroy K, Bégard S, Brion J-P, Hamdane M, Buée L (2006) Alzheimer's disease-like tau neuropathology leads to memory deficits and loss of functional synapses in a novel mutated tau transgenic mouse without any motor deficits. *Am J Pathol* **169**, 599-616.

[37] Scattoni ML, Gasparini L, Alleva E, Goedert M, Calamandrei G, Spillantini MG (2010) Early behavioural markers of disease in P301S tau transgenic mice. *Behav Brain Res* **208**, 250-257.

[38] Allen B, Ingram E, Takao M, Smith MJ, Jakes R, Virdee K, Yoshida H, Holzer M, Craxton M, Emson PC, Atzori C, Migheli A, Crowther RA, Ghetti B, Spillantini MG, Goedert M (2002) Abundant tau filaments and nonapoptotic neurodegeneration in transgenic mice expressing human P301S tau protein. *J Neurosci* **22**, 9340-9351.

[39] Terwel D, Lasrado R, Snauwaert J, Vandeweert E, Van Haesendonck C, Borghgraef P, Van Leuven F (2005) Changed conformation of mutant tau-P301L underlies the moribund tauopathy, absent in progressive, nonlethal axonopathy of tau-4R/2N transgenic mice. *J Biol Chem* **280**, 3963-3973.

[40] Gonzalez-Freire M, de Cabo R, Studenski SA, Ferrucci L (2014) The neuromuscular junction: Aging at the crossroad between nerves and muscle. *Front Aging Neurosci* **6**, 208.

[41] Pratt SJP, Shah SB, Ward CW, Inacio MP, Stains JP, Lovering RM (2013) Effects of in vivo injury on the neuromuscular junction in healthy and dystrophic muscles. *J Physiol* **591**, 559-570.

[42] Ling KKY, Gibbs RM, Feng Z, Ko C-P (2012) Severe neuromuscular denervation of clinically relevant muscles in a mouse model of spinal muscular atrophy. *Hum Mol Genet* **21**, 185-195.

[43] Moloney EB, de Winter F, Verhaagen J (2014) ALS as a distal axonopathy: Molecular mechanisms affecting neuromuscular junction stability in the presymptomatic stages of the disease. *Front Neurosci* **8**, 252.

[44] Dadon-Nachum M, Melamed E, Offen D (2011) The "dying-back" phenomenon of motor neurons in ALS. *J Mol Neurosci* **43**, 470-477.

[45] Boido M, Vercelli A (2016) Neuromuscular junctions as key contributors and therapeutic targets in spinal muscular atrophy. *Front Neuroanat* **10**, 1-10.

[46] Zesiewicz TA, Baker MJ, Dunne PB, Hauser RA (2001) Diffuse Lewy body disease. *Curr Treat Options Neurol* **3**, 507-518.

[47] Bennett GJ, Liu GK, Xiao WH, Jin HW, Siau C (2011) Terminal arbor degeneration–a novel lesion produced by the antineoplastic agent paclitaxel. *Eur J Neurosci* **33**, 1667-1676.

[48] Shi P, Gal J, Kwinter DM, Liu X, Zhu H (2010) Mitochondrial dysfunction in amyotrophic lateral sclerosis. *Biochim Biophys Acta* **1802**, 45-51.

[49] Reddy PH (2011) Abnormal tau, mitochondrial dysfunction, impaired axonal transport of mitochondria, and synaptic deprivation in Alzheimer's disease. *Brain Res* **1415**, 136-148.

[50] Chang DTW, Honick AS, Reynolds IJ (2006) Mitochondrial trafficking to synapses in cultured primary cortical neurons. *J Neurosci* **26**, 7035-7045.

[51] Dawson HN, Cantillana V, Jansen M, Wang H, Vitek MP, Wilcock DM, Lynch JR, Laskowitz DT (2010) Loss of tau elicits axonal degeneration in a mouse model of Alzheimer's disease. *Neuroscience* **169**, 516-531.

[52] Smith KDB, Kallhoff V, Zheng H, Pautler RG (2007) In vivo axonal transport rates decrease in a mouse model of Alzheimer's disease. *Neuroimage* **35**, 1401-1408.

[53] Sanchez-Varo R, Trujillo-Estrada L, Sanchez-Mejias E, Torres M, Baglietto-Vargas D, Moreno-Gonzalez I, De Castro V, Jimenez S, Ruano D, Vizuete M, Davila JC, Garcia-Verdugo JM, Jimenez AJ, Vitorica J, Gutierrez A (2012) Abnormal accumulation of autophagic vesicles correlates with axonal and synaptic pathology in young Alzheimer's mice hippocampus. *Acta Neuropathol* **123**, 53-70.

[54] Stamer K, Vogel R, Thies E, Mandelkow E, Mandelkow EM (2002) Tau blocks traffic of organelles, neurofilaments, and APP vesicles in neurons and enhances oxidative stress. *J Cell Biol* **156**, 1051-1063.

[55] Mandelkow EM, Stamer K, Vogel R, Thies E, Mandelkow E (2003) Clogging of axons by tau, inhibition of axonal traffic and starvation of synapses. *Neurobiol Aging* **24**, 1079-1085.

[56] Vossel KA, Zhang K, Brodbeck J, Daub AC, Sharma P, Finkbeiner S, Cui B, Mucke L (2010) Tau reduction prevents Abeta-induced defects in axonal transport. *Science* **330**, 198.

[57] Mizisin AP, Shelton GD, Wagner S, Rusbridge C, Powell HC (1998) myelin splitting, Schwann cell injury and demyelination in feline diabetic neuropathy. *Acta Neuropathol* **95**, 171-174.

[58] de Waegh S, Brady ST (1990) Altered slow axonal transport and regeneration in a myelin-deficient mutant mouse: The trembler as an in vivo model for Schwann cell-axon interactions. *J Neurosci* **10**, 1855-1865.

[59] Schneider A, Araújo GW, Trajkovic K, Herrmann MM, Merkler D, Mandelkow EM, Weissert R, Simons M (2004) Hyperphosphorylation and aggregation of tau in experimental autoimmune encephalomyelitis. *J Biol Chem* **279**, 55833-55839.

[60] Anderson JM, Hampton DW, Patani R, Pryce G, Crowther RA, Reynolds R, Franklin RJM, Giovannoni G, Compston DAS, Baker D, Spillantini MG, Chandran S (2008) Abnormally phosphorylated tau is associated with neuronal and axonal loss in experimental autoimmune encephalomyelitis and multiple sclerosis. *Brain* **131**, 1736-1748.

[61] Kirkpatrick L, Brady T, Biology C, Southwestern T (1994) Modulation of the axonal Schwann cells microtubule cytoskeleton by myelinating. *J Neurosci* **14**, 7440-7450.

[62] Lisney SJ (1989) Regeneration of unmyelinated axons after injury of mammalian peripheral nerve. *Q J Exp Physiol* **74**, 757-784.

[63] Jessen KR, Mirsky R (2016) The repair Schwann cell and its function in regenerating nerves. *J Physiol* **594**, 3521-3531.

[64] Arthur-Farraj PJ, Latouche M, Wilton DK, Quintes S, Chabrol E, Banerjee A, Woodhoo A, Jenkins B, Rahman M, Turmaine M, Wicher GK, Mitter R, Greensmith L, Behrens A, Raivich G, Mirsky R, Jessen KR (2012) c-Jun reprograms Schwann cells of injured nerves to generate a repair cell essential for regeneration. *Neuron* **75**, 633-647.

[65] Vickland H, Silver J (1997) The role of astrocytes in axon guidance during development and repair. In Glial Cell Development: Basic principles and clinical relevance, Jessen KR, Richardson WD, eds. Oxford, BIOS Scientific Publishers, Herndon, VA, pp. 197-208.

[66] Sasaki A, Kawarabayashi T, Murakami T, Matsubara E, Ikeda M, Hagiwara H, Westaway D, George-Hyslop PS, Shoji M, Nakazato Y (2008) Microglial activation in brain lesions with tau deposits: Comparison of human tauopathies and tau transgenic mice TgTauP301L. *Brain Res* **1214**, 159-168.

[67] Rotshenker S (2009) The role of Galectin-3/MAC-2 in the activation of the innate-immune function of phagocytosis in microglia in injury and disease. *J Mol Neurosci* **39**, 99-103.

[68] Nguyen JV, Soto I, Kim K-Y, Bushong EA, Oglesby E, Valiente-Soriano FJ, Yang Z, Davis CO, Bedont JL, Son JL, Wei JO, Buchman VL, Zack DJ, Vidal-Sanz M, Ellisman MH, Marsh-Armstrong N (2011) Myelination transition zone astrocytes are constitutively phagocytic and have synuclein dependent reactivity in glaucoma. *Proc Natl Acad Sci U S A* **108**, 1176-1181.

[69] Reichert F, Saada A, Rotshenker S (1994) Peripheral nerve injury induces Schwann cells to express two macrophage phenotypes: Phagocytosis and the galactose-specific lectin MAC-2. *J Neurosci* **14**, 3231-3245.